Two-Dimensional Assembling of (2,2′-Bipyrimidine)bis(oxalato)chromate(III) Units through Alkaline Cations

Giovanni De Munno,*,† Donatella Armentano,† Miguel Julve,*,‡ Francesc Lloret,‡ Rodrigue Lescouëzec,‡ and Juan Faus‡

Dipartimento di Chimica della Università degli Studi della Calabria, 87030 Arcavacata di Rende, Cosenza, Italy, and Departament de Química Inorgànica, Facultat de Química de la Universitat de València, Dr. Moliner 50, 46100 Burjassot (València), Spain

Received October 20, 1998

Introduction

The recent but extensive use of the tris(oxalato)chromate(III) anion ($[Cr(ox)_3]^{3-}$) as "complex ligand" toward first-row transition metal ions has afforded two- (2D)[1−6] and three- (3D)[7,8] dimensional oxalato-bridged homo- and heterometallic assemblies exhibiting very interesting magnetic and/or photophysical properties.[1−9] It has been found that the formation of either a 2D or a 3D oxalato-bridged structure depends on the nature of the template counterion. So, layered structures containing $[M^{II}M^{III}(ox)_3]_n^{n-}$ units are obtained when $[XR_4]^+$ (X = N, P; R = alkyl group) is used as a cation, whereas 3D networks of formula $[M^{II}_2(ox)_3]_n^{2n-}$, $[M^{I}M^{III}(ox)_3]_n^{2n-}$, or $[M^{II}M^{III}(ox)_3]_n^{n-}$ result when the charge is counterbalanced by tris-chelated transition-metal diimine $[M(bpy)_3]^{m+}$ (bpy = 2,2′-bipyridine; $m = 2, 3$).[9] Within the oxalate-bridged network, building blocks of opposite chirality are alternatively linked in the 2D family whereas they exhibit the same enantiomeric form in the 3D one.

In previous works, we have shown how the simultaneous use of two bis-chelating ligands such as oxalate and 2,2′-bipyrimidine (bpm) allows the rational synthesis of homometallic honeycomb layered materials of formula $[M_2(bpm)(ox)_2]\cdot nH_2O$, M being either Cu(II) with $n = 5$ (**3**) or Mn(II) with $n = 6$ (**4**).[10,11] During the preparation of inert Cr(III) anionic precursors containing these ligands, we have noticed that the counterion not only counterbalances the charge of the anion and allows the crystallization of the desired salt but also is involved as a structural element. This is the case for the first mononuclear and sheetlike bpm- and ox-containing chromium(III) complexes of formula $AsPh_4[Cr(bpm)(ox)_2]\cdot H_2O$ (**1**) and $[NaCr(bpm)(ox)_2]\cdot 5H_2O$ (**2**), respectively. Their preparation, crystal structure, and magnetic properties are presented.

Experimental Section

Materials. 2,2′-Bipyrimidine, chromium(III) chloride hexahydrate, sodium oxalate, lithium hydroxide monohydrate, oxalic acid dihydrate, and tetraphenylarsonium chloride were purchased from commercial sources and used as received. Elemental analysis (C, H, N) were conducted by the Microanalytical Service of the Universidad Autónoma de Madrid. Metal contents were determined by absorption spectrometry.

Preparation of $AsPh_4[Cr(bpm)(ox)_2]\cdot H_2O$ (1). An aqueous solution (60 cm^3) containing chromium(III) chloride (2 mmol), bpm (2 mmol), and lithium oxalate (4 mmol) was refluxed under continuous stirring until the initial green color turned reddish violet (∼1 h). The addition of tetraphylarsonium chloride monohydrate (2 mmol) dissolved in a mimimum amount of water caused the crystallization of **1** as reddish violet parallelepipeds. Yield ∼90%. Anal. Calcd for $C_{36}H_{28}AsCrN_4O_9$ (**1**): C, 54.91; H, 3.56; N, 7.11. Found: C, 54.83; H, 3.45; N, 7.02.

Preparation of $[NaCr(bpm)(ox)_2]\cdot 5H_2O$ (2). The preparation of **2** is similar to that of **1** except that lithium oxalate is replaced by its sodium salt. **2** was obtained as pink violet rhombuses by slow evaporation of the aqueous solution at room temperature. Because of the great solubility of **2** in water, high yields require evaporation nearly to dryness. Anal. Calcd for $C_{12}H_{16}CrN_4NaO_{13}$ (**2**): C, 28.87; H, 3.21; N, 11.22; Cr, 10.42; Na, 4.61. Found: C, 28.65; H, 3.17; N, 11.08; Cr, 10.30; Na, 4.53.

The ring stretching mode of bpm appears as quasi-symmetric (1575 and 1545 cm^{-1}, **1**) and very asymmetric (1580 and 1550 cm^{-1}, **2**) doublets in agreement with the presence of chelating (**1**) and bis-chelating (**2**) bpm.[12] For the oxalate ligand, significant differences are observed in the ν_{as}(CO) (three strongs peaks at 1710, 1700, and 1675 cm^{-1} for **1** and two strong absorptions at 1710 and 1675 cm^{-1} for **2**) and ν_s(CO) (a triplet centered at 1360 cm^{-1} for **1** and a single absorption at 1355 cm^{-1} for **2**) ranges. The different coordination modes adopted by the oxalate in **1** (bidentate) and **2** (bis-bidentate) account for these spectral features.

Physical Techniques. IR spectra were recorded on a Nicolet Impact 410 spectrophotometer as KBr pellets in the 4000−400-cm^{-1} region. Magnetic susceptibility measurements were carried out on polycrystalline samples in the temperature range 2−300 K under a magnetic field of 0.1 T by using a Quantum Design SQUID magnetometer. The susceptometer was calibrated with $(NH_4)_2Mn(SO_4)_2\cdot 12H_2O$. The corrections for the diamagnetism using Pascal's constants were -401×10^{-6} and -234×10^{-6} $cm^3\ mol^{-1}$ for complexes **1** and **2**, respectively.

X-ray Data Collection and Structure Refinement. Diffraction data were collected at room temperature on a Siemens R3m/V automatic diffractometer by using graphite-monochromatized Mo Kα radiation

* To whom correspondence should be addressed.
† Dipartimento di Chimica Inorganica, Università degli Studi della Calabria.
‡ Departament de Química Inorgànica, Universitat de València.

(1) Tamaki, H.; Zhong, Z. J.; Matsumoto, N.; Kida, S.; Koikawa, M.; Achiwa, N.; Hashimoto, Y.; Okawa, H. *J. Am. Chem. Soc.* **1992**, *114*, 6974.
(2) Atovmyan, L. O.; Shilov, G. V.; Lyubobskaya, R. N.; Zhilyaeva, E. I.; Ovanesyan, N. S.; Pirumova, S. I:; Gusakovskaya, I. G. *JETP Lett.* **1993**, *58*, 766.
(3) (a) Decurtins, S.; Schmalle, H. W.; Oswald, H. R.; Linden, A.; Ensling, J.; Gütlich, P.; Hauser, A. *Inorg. Chim. Acta* **1994**, *216*, 65. (b) Pelleaux, R.; Schmalle, H. W.; Huber, R.; Fischer, P.; Hauss, T.; Ouladdiaf, B.; Decurtins, S. *Inorg. Chem.* **1997**, *36*, 2301.
(4) Reiff, W. M.; Kreisz, J.; Meda, L.; Kirss, R. U. *Mol. Cryst. Liq. Cryst.* **1995**, *273*, 181.
(5) Farrell, R. P.; Hambley, T. W.; Lay, P. A. *Inorg. Chem.* **1995**, *34*, 757.
(6) (a) Mathonière, C.; Nuttall, C. J.; Carling, S. G.; Day, P. *Inorg. Chem.* **1996**, *35*, 1201. (b) Carling, S. G.; Mathonière, C.; Day, P.; Malik, K. M. A.; Coles, S. J.; Hursthouse, M. B. *J. Chem. Soc., Dalton Trans.* **1996**, 1839.
(7) (a) Decurtins, S.; Schmalle, H. W.; Schneuwly, P.; Oswald, H. R. *Inorg. Chem.* **1993**, *32*, 1888. (b) Decurtins, S.; Schmalle, H. W.; Schneuwly, P.; Ensling, J.; Gütlich, P. *J. Am. Chem. Soc.* **1994**, *116*, 9521. (c) Decurtins, S.; Schmalle, H. W.; Pellaux, R.; Schneuwly, P.; Hauser, A. *Inorg. Chem.* **1996**, *35*, 1451. (d) Decurtins, S.; Schmalle, H. W.; Pellaux, R.; Huber, R.; Fischer, P.; Ouladdiaf, B. *Adv. Mater.* **1996**, *8*, 647.
(8) Hernández-Molina, M.; Lloret, F.; Ruiz-Pérez, C.; Julve, M. *Inorg. Chem.* **1998**, *37*, 4131.
(9) Decurtins, S.; Schmalle, H. W.; Pellaux, R.; Fischer, P.; Hauser, A. *Mol. Cryst. Liq. Cryst.* **1997**, *305*, 227.
(10) De Munno, G.; Julve, M.; Nicolò, F.; Lloret, F.; Faus, J.; Ruiz, R.; Sinn, E. *Angew. Chem., Int. Ed. Engl.* **1993**, *32*, 795.
(11) De Munno, G.; Ruiz, R.; Lloret, F.; Faus, J.; Sessoli, R.; Julve, M. *Inorg. Chem.* **1995**, *34*, 408.
(12) Julve, M.; Verdaguer, M.; De Munno, G.; Real, J. A.; Bruno, G. *Inorg. Chem.* **1993**, *32*, 795.

10.1021/ic981232q CCC: $18.00
Published on Web 04/07/1999

Table 1. Crystallographic Data for $AsPh_4[Cr(bpm)(ox)_2]\cdot H_2O$ (**1**) and $[NaCr(bpm)(ox)_2]\cdot 5H_2O$ (**2**)

compound	**1**	**2**
formula	$C_{36}H_{28}AsCrN_4O_9$	$C_{12}H_{16}CrN_4NaO_{13}$
fw	787.5	499.2
space group	$P2_1/c$	$C2$
a, Å	14.628(4)	9.886(3)
b, Å	13.787(4)	17.388(5)
c, Å	18.084(5)	6.029(2)
β, deg	112.46(2)	103.33(2)
V, Å^3	3370.5(16)	1008.4(5)
Z	4	2
T, K	295	295
ρ_{calcd}, g cm^{-3}	1.552	1.611
λ, Å	0.710 73	0.710 73
μ(Mo Kα), cm^{-1}	13.77	6.62
R^a	0.061	0.048
$R_w{}^b$	0.061	0.049

^{a} $R = \sum(||F_o| - |F_c||)/\sum|F_o|$. ^{b} $R_w = [\sum w(||F_o| - |F_c||)^2/\sum w|F_o|^2]^{1/2}$.

and the $\omega-2\theta$ scan technique. Unit cell dimensions and crystal orientation matrixes were obtained from least-squares refinement of 25 strong reflections in the $15 \le \theta \le 30°$ range. A summary of the crystallographic data and structure refinement is given in Table 1. Totals of 8365 (**1**) and 2630 (**2**) reflections were collected in the range $3 \le 2\theta \le 54°$; 7397 (**1**) and 2225 (**2**) of them were unique, and from these, 3603 (**1**) and 2159 (**2**) were assumed as observed ($I > 3\sigma(I)$). Examination of three standard reflections, monitored after every 100, showed no sign of crystal deterioration. Lorentz polarization (**1** and **2**) and ψ-scan absorption (**1**) corrections[13] were applied to the intensity data. The maximum and minimum transmission factors were 0.866 and 0.497 for **1** and 0.892 and 0.569 for **2**.

The structures of **1** and **2** were solved by standard Patterson methods with the SHELXTL PLUS program[14] and subsequently completed by Fourier recycling. All non-hydrogen atoms were refined anisotropically. The hydrogen atoms of the water molecules of **1** were located on a ΔF map and refined with constraints where those of the water molecules of **2** were not located. The hydrogen atoms of the bpm ligand were set in calculated positions and refined as riding atoms. They were all refined isotropically. The final full-matrix least-squares refinement on F^2, minimizing the function $\sum w(|F_o| - |F_c|)^2$ with $w = 1/[\sigma^2(F_o) + q(F_o)^2]$ ($q = 0.0010$ for **1** and 0.0050 for **2**), converged to final residuals R (R_w) of 0.061 (0.061) for **1** and 0.048 (0.049) for **2**. The goodness of fit values were 1.691 (**1**) and 0.889 (**2**). Residual maximums and minimums in the final difference map were 0.77 and -0.58 e Å^{-3} for **1** and 1.80 and -1.93 e Å^{-3} for **2**. The final geometrical calculations and graphical manipulations were carried out with the PARST program[15] and XP utility of the SHELX-PLUS system, respectively. Selected bond distances and angles are gathered in Tables 2 (**1**) and 3 (**2**).

Results and Discussion

Description of the Structures. Preparation of $AsPh_4[Cr(bpm)(ox)_2]\cdot H_2O$ (1). The crystal structure of **1** consists of mononuclear $[Cr(bpm)(ox)_2]^-$ anions (Figure 1), tetraphenylarsonium cations, and uncoordinated water molecules. Each chromium atom is six-coordinated with two bpm nitrogen and four oxalate oxygen atoms building a distorted octahedral environment. The mean values of the Cr−N and Cr−O bond distances are 2.075(6) and 1.945(6) Å, respectively. The former mean value is practically identical to that observed in the chelating bpm−chromium(III) complex of formula $NEt_4[Cr(bpm)(NCS)_4]$ [2.072(3) Å][16] whereas the latter one is somewhat shorter than that reported in $K_3[Cr(ox)_3]\cdot 3H_2O$ [1.969(13) Å][17] but within the range reported for terminal oxalate in $(NBu_4)_4[Cr_2(ox)_5]\cdot 2CHCl_3$ [1.925(2)−1.923(7) Å].[18] As expected for bidentate bpm and ox ligands, the values of the bite angle are considerably less than 90° [78.2(3), 83.5(3), and 82.8(2)° for N(1)−Cr(1)−N(4), O(1)−Cr(1)−O(2), and O(5)−Cr(1)−O(6), respectively]. The bpm ligand as a whole is nearly planar and it forms dihedral angles of 91.3(2) and 86.6(2)° with the oxalate mean planes. Two sets of oxalate carbon−oxygen bond distances are observed, the shorter values belonging to the peripheral C−O bonds in agreement with its greater double bond character [the ranges of the values for peripheral and inner C−O bonds are

Table 2. Selected Bond Lengths (Å) and Angles (deg)[a] for Compound **1**

Cr(1)−N(1)	2.081(7)	Cr(1)−N(4)	2.069(6)
Cr(1)−O(1)	1.956(5)	Cr(1)−O(2)	1.931(6)
Cr(1)−O(5)	1.947(6)	Cr(1)−O(6)	1.945(6)
N(1)−Cr(1)−N(4)	78.2(3)	N(1)−Cr(1)−O(1)	93.8(2)
N(4)−Cr(1)−O(1)	170.0(3)	N(1)−Cr(1)−O(2)	90.8(3)
N(4)−Cr(1)−O(2)	90.6(3)	O(1)−Cr(1)−O(2)	83.5(3)
N(1)−Cr(1)−O(5)	90.1(3)	N(4)−Cr(1)−O(5)	90.0(3)
O(1)−Cr(1)−O(5)	96.0(3)	O(2)−Cr(1)−O(5)	179.0(2)
N(1)−Cr(1)−O(6)	168.8(2)	N(4)−Cr(1)−O(6)	93.1(2)
O(1)−Cr(1)−O(6)	95.5(2)	O(2)−Cr(1)−O(6)	96.5(2)
O(5)−Cr(1)−O(6)	82.8(2)		

[a] Estimated standard deviations in the last significant digits are given in parentheses.

Table 3. Selected Bond Lengths (Å) and Angles (deg)[a,b] for Compound **2**

Cr(1)−N(1)	2.067(3)	Cr(1)−O(1)	1.953(2)
Cr(1)−O(2)	1.962(2)	Na(1)−N(2)	2.489(4)
Na(1)−O(4b)	2.356(3)	Na(1)−O(3b)	2.407(4)
N(1)−Cr(1)−O(1)	93.7(1)	N(1)−Cr(1)−O(2)	94.1(1)
O(1)−Cr(1)−O(2)	83.2(1)	N(1)−Cr(1)−N(1a)	78.7(1)
O(1)−Cr(1)−N(1a)	88.6(1)	O(2)−Cr(1)−N(1a)	168.7(1)
O(1)−Cr(1)−O(1a)	177.1(2)	O(2)−Cr(1)−O(1a)	94.8(1)
O(2)−Cr(1)−O(2a)	94.2(1)	N(2)−Na(1)−N(2a)	68.2(2)
N(2)−Na(1)−O(4c)	157.4(1)	N(2)−Na(1)-O(4b)	100.8(1)
O(4c)−Na(1)−O(4b)	95.7(2)	N(2)−Na(1)−O(3c)	89.9(1)
N(2)−Na(1)−O(3b)	97.3(1)	O(4c)−Na(1)−O(3b)	102.6(1)
O(4b)−Na(1)−O(3b)	71.4(1)	O(3c)-Na(1)−O(3b)	171.3(2)

[a] Estimated standard deviations in the last significant digits are given in parentheses. [b] Symmetry code: (a) $-x, y, -z$; (b) $0.5 - x, -0.5 + y, -z$; (c) $-0.5 + x, -0.5 + y, z$; (d) $0.5 + x, 0.5 + y, z$.

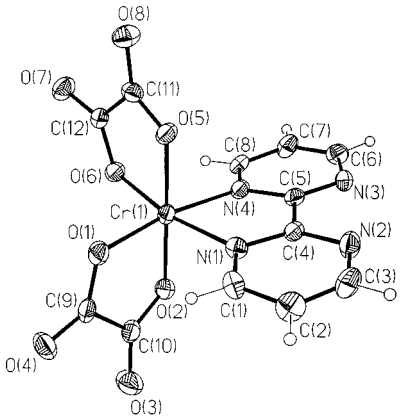

Figure 1. Perspective drawing of the $[Cr(bpm)(ox)_2]^-$ mononuclear unit of **1**. Thermal ellipsoids are drawn at the 30% probability level.

(13) North, A. C. T.; Philips, D. C.; Mathews, F. S. *Acta Crystallogr.* **1968**, *A24*, 351.
(14) SHELX-PLUS, Version 4.21/V.; Siemens Analytical X-Ray Instruments Inc.: Madison, WI, 1990.
(15) Nardelli, M. *Comput. Chem.* **1983**, *7*, 95.
(16) Garland, M. T.; Baggio, R. F.; Bérézovsky, F.; Triki, S.; Sala Pala, J. *Acta Crystallogr.* **1997**, *C53*, 1803.
(17) Taylor, D. *Aust. J. Chem.* **1978**, *31*, 1455.
(18) Masters, V. M.; Sharrad, C. A.; Bernhardt, P. V.; Gahan, L. R.; Moubaraki, B.; Murray, K. *S. J. Chem. Soc., Dalton Trans.* **1998**, 413.

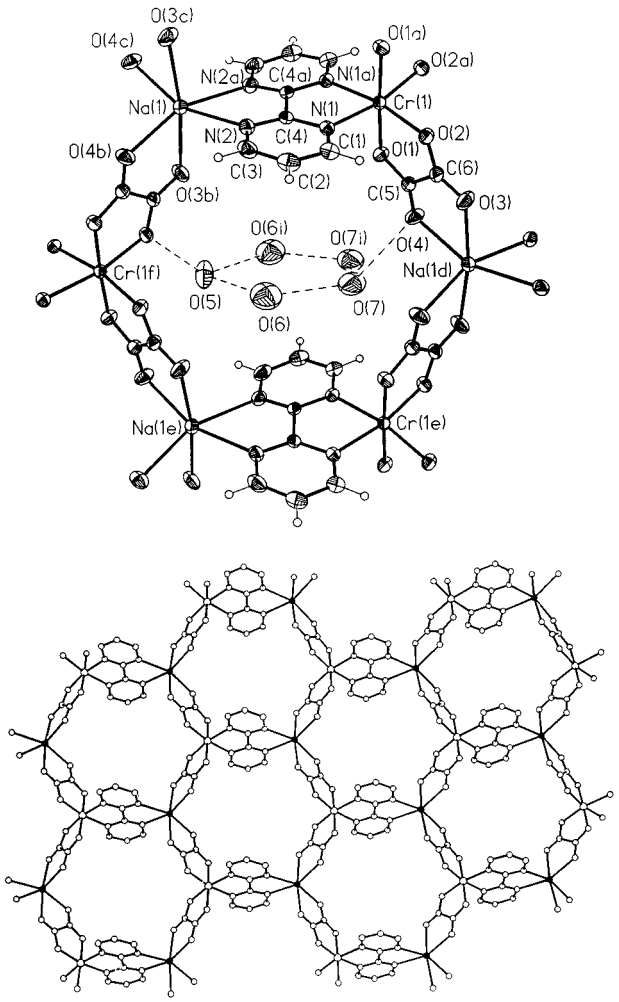

Figure 2. View of the structure of **2** (ellipsoids at the 30% probability level). (top) $[Cr^{III}_3Na^{I}_3]$ hexanuclear repeating ring with the atom numbering (hydrogen bonds within the ring are illustrated by broken lines); (bottom) a sheet of **2** extending in the *xy* plane that shows the chicken wire arrangement adopted by the Cr^{III} (○) and Na^{I} (●) ions (hydrogen atoms and water molecules have been omitted for the sake of clarity).

1.202(12)−1.223(11) and 1.289(11)−1.306(11) Å, respectively]. The uncoordinated water molecules form hydrogen bonds with two oxalate oxygens [2.94(1) Å and 140(1)° for O(9)···O(8) and O(9)−H(1w)···O(8) and 2.96(1) Å and 143(1)° for O(9)···O(3a) and O(9)−H(2w)···O(3a); (a) = $-x$, $-0.5 + y$, $1.5 - z$]. The mononuclear units are well separated from each other by the bulky tetrahedral $AsPh_4^+$ cation, the shortest intermolecular Cr(1)···Cr(1a) separation being 7.254(3) Å.

$[NaCr(bpm)(ox)_2]\cdot 5H_2O$ (2). The crystal structure of **2** is made up of parallel sheets each consisting of an infinite hexagonal array of chromium and sodium atoms bridged by bis-bidentate ox and bpm ligands (Figure 2). Clusters of water molecules are also present. This structure is similar to those of **3** and **4** apart from the substitution of two copper(II) (**3**) or two manganese(II) (**4**) ions by a Cr(III)−Na(I) pair and the number of hydratation water molecules (five in **2** and **3** and six in **4**). Both metal atoms in **2** are six-coordinated MN_2O_4. The M−N bond lengths [2.067(3) and 2.489(4) Å for Cr−N and Na−N] are longer than the M−O ones [1.957(2) and 2.381(3) Å for Cr−O and Na−O]. These latter values are in agreement with those reported for the oxalato-bridged 3D compound of formula $[Cr^{III}(bpy)_3][Na^{I}Cr^{III}(ox)_3]ClO_4$ [1.964(4) and 1.956(4) Å for Cr−O and 2.342(5) and 2.320(6) Å for Na−O].[7c] The most

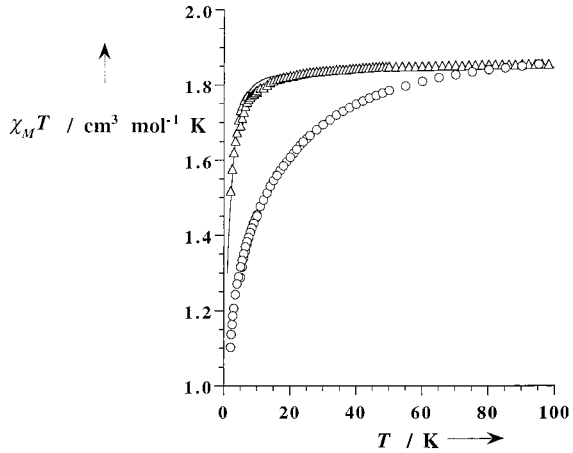

Figure 3. $\chi_M T$ versus T plot for **1** (△) and **2** (○). The solid line in **1** is the best-fit curve (see text).

significant distortions from the ideal octahedral geometry around the chromium and sodium atoms arise from the reduced values of the bite of the bpm [79.7(1) and 68.2(2)°] and ox [83.2(1) and 71.4(1)°] ligands. The bpm group is almost planar and it forms dihedral angles of 97.8(1) and 65.8(1)° with the oxalate and sheet planes, respectively. As shown in Figure 2, almost circular rings are formed in the *xy* plane. The intra-ring Cr···Na distances are 6.025(3) [Cr(1)···Na(1)], 5.618(2) [Cr(1)···Na(1d), (d) = $0.5 + x$, $0.5 + y$, z], 11.577(3) [Cr(1)···Na(1e), (e) = $1 + x$, y, z], and 11.363(2) Å [Cr(1f)···Na(1d), (f) $0.5 + x$, $-0.5 + y$, z]. The intra-ring Cr···Cr and Na···Na separations are 9.886(3) [Cr(1)···Cr(1e) and Na(1)···Na(1e)] and 10.001(3) Å [Cr(1)···Cr(1f) and Na(1)···Na(1d)]. The layers are superposed along the *z* axis and they are stacked by graphitelike interactions between the bpm rings [the separation between two bpm molecules of two adjacent layers is 3.671(2) Å]. The five water molecules, which are accommodated in each hexagonal hole of the sheets, are linked together by means of hydrogen bonds [2.979(10), 2.825(12), and 2.723(12) Å for O(5)···O(6) (and O(5)···O(6i)), O(6)···O(7), and O(7)···O(7i), respectively; (i) = $1 - x$, y, $-1 - z$] to form a planar ring. These rings form a dihedral angle of 98.3(1)° with the sheet plane. Rings of parallel sheets are linked together through hydrogen bonds involving the O(6), O(6r), O(6i), and O(6s) atoms [2.673(13) Å for O(6)···O(6r) and O(6i)···O(6s); (r) = $1 - x$, y, $-z$; (s) = x, y, $-1 + z$], to form columns propagating along the *z* axis.

These columns are inserted into the channels delimited by the cavities and are attached to the wall of the channels by hydrogen bonds through O(5) and O(7) oxygen atoms [2.944(4) Å for O(5)···O(2b) and O(5)···O(2 g) and 2.984(8) Å for O(7)···O(4) and O(7i)···O(4i); (b) = $0.5 - x$, $-0.5 + y$, $-z$; (g) $0.5 + x$, $-0.5 + y$, $-1 + z$].

Magnetic Properties of 1 and 2. The temperature dependence of $\chi_M T$ for **1** and **2** [χ_M is the magnetic susceptibility per mole of chromium(III)] in the temperature range 2.0−100 K is shown in Figure 3. At room temperature, the $\chi_M T$ value (∼1.87 cm^3 mol^{-1} K) is practicaly identical for both compounds and it is as expected for a magnetically isolated $S = {}^3/_2$ quartet. This value remains practically constant when cooling and it decreases smoothly in the lower temperature region (the $\chi_M T$ values for **1** and **2** at 2.0 K are 1.52 and 1.10 cm^3 mol^{-1} K, respectively), the $\chi_M T$ data of **2** being significantly smaller than those of **1**. No susceptibility maximum was observed in the temperature range explored. The magnetic data of **1** have been analyzed through the appropriate equation for a mononuclear chromium(III) complex, the variable parameters being g (Landé factor)

and D (zero-field splitting parameter).[19] A satisfactory fit of the magnetic data was obtained with $g = 1.98$, $D = |2.7|$ cm^{-1}, and $R = 1.6 \times 10^{-5}$ (R = agreement factor = $\sum_i[(\chi_M T)_{obs}(i) - (\chi_M T)_{calc}(i)]^2/\sum_i[(\chi_M T)_{obs}(i)]^2$). The values of $\chi_M T$ for **2** decrease faster than those of **1**. All our attempts to fit the $\chi_M T$ values of **2** to the same expression used for that of **1** even including a θ-parameter (intermolecular interactions) were unsuccessful. These features strongly suggest the occurrence of an antiferromagnetic exchange coupling between the chromium(III) centers in **2**. This is quite surprising because although the structure of **2** corresponds to an alternating magnetic plane containing very efficient exchange mediators (bpm and ox) as bridging ligands,[11,12,18,20−24] the Cr···Cr separation through the ox−Na−bpm and ox−Na−ox bridging pathways is very large (∼10 Å). At this point, it should to be noted that the value of the exchange coupling between two Cr(III) ions bridged by oxalato in the $[Cr_2(ox)_5]^{4-}$ dinuclear complex is $J = -6.2$ cm^{-1}, the metal−metal separation being 5.32 Å.[18] Neither structural nor magnetic data concerning bpm-bridged chromium(III) complexes are available to the best of our knowledge. In a recent paper,[25] a weak intralayer antiferromagnetic interaction between Cr(III) ions bridged by bpm, ox, and K^+ in the sheetlike compound $[KCr(bpm)(ox)_2(H_2O)]$ (**5**) was reported. In this case, the resulting sheetlike structure shows a tetragonal array of six-coordinated Cr(III) and eight-coordinated K(I) cations. Unfortunately, the lack of a theoretical model to treat the magnetic data of the alternating ox and bpm heterometallic honeycomb complex **2** (or **5**) with a local spin $S = {}^3/_2$ precludes a thorough analysis.

In recent work, it has been shown how the sodium cation can act as a nucleation center in the preparation of discrete heterometallic species,[26] the highest nuclearity being represented by the $[Ni^{II}_{16}Na^{I}_6]$ supracage assembly.[27] Here we show how the coordination of sodium by a tris-chelated 3d metal complex (**1**) appears as a useful strategy in designing two-dimensional bimetallic compounds such as **2** where the chromium and sodium atoms exhibit a perfect alternation of opposite enantiomeric forms within each layer. Finally, it deserves to be noted that the present work illustrates how the choice of the cation (tetraphenylarsonium in **1** and sodium in **2**) can lead either to mononuclear (**1**) or sheetlike (**2**) compounds.

Acknowledgment. Financial support from the Spanish Dirección General de Investigación Científica y Técnica (DGICYT) through Project PB97-1397, the Italian Ministero dell'Università e della Ricerca Scientifica e Tecnologica, and the TMR Program from the European Union (Contract ERBFMRXCT98-0181) is gratefully acknowledged.

Supporting Information Available: Tables of crystal data, anisotropic displacement parameters for non-hydrogen atoms, atomic fractional coordinates, nonessential bond lengths and angles and least-squares planes for **1** and **2**. X-ray crystallographic files in CIF format for **1** and **2** are also available. This material is available free of charge via the Internet at http://pubs.acs.org.

IC981232Q

(19) O'Connor, C. J. *Prog. Inorg. Chem.* **1986**, *29*, 203.
(20) De Munno, G.; Julve, M. In *Metal Ligand Interactions. Structure and Reactivity*; Russo, N., Salahub, D. R., Eds.; NATO ASI Series C 474; Kluwer: Dordrecht, 1996; p 139.
(21) Julve, M.; Verdaguer, M.; Gleizes, A.; Philoche-Levisalles, M.; Kahn, O. *Inorg. Chem.* **1984**, *23*, 3808.
(22) Alvarez, S.; Julve, M.; Verdaguer, M. *Inorg. Chem.* **1990**, *29*, 4500.
(23) Glerup, J.; Goodson, P. A.; Hodgson, D. J.; Michelsen, K. *Inorg. Chem.* **1995**, *34*, 6255.
(24) Román, P.; Guzmán-Miralles, C.; Luque, A.; Beitia, J. I.; Cano, J.; Lloret, F.; Julve, M.; Alvarez, S. *Inorg. Chem.* **1996**, *35*, 3741.
(25) Bérézovsky, F.; Hajem, A. A.; Triki, S.; Sala Pala, J., Molinié, P. *Inorg. Chim. Acta* **1998**, *284*, 8.
(26) Brechin, E. K.; Gilby, L. M.; Gould, R. O.; Harris, S. G.; Parsons, S.; Winpenny, R. E. P. *J. Chem. Soc., Dalton Trans.* **1998**, 2657 and references therein.
(27) Brechin, E. K.; Gould, R. O.; Harris, S. G.; Parsons, S.; Winpenny, R. E. P. *J. Am. Chem. Soc.* **1996**, *118*, 11293.